16th World Conference on Earthquake, 16WCEE 2017

Santiago Chile, January 9th to 13th 2017

Paper N° 376

Registration Code: S-X1461982603

USE OF SHAKING TABLE TESTS TO OBTAIN OPTIMAL DAMPER CHARACTERISTICS OF PASSIVE VIBRATION CONTROL STRUCTURES CONSIDERING SOIL–STRUCTURE INTERACTION

K. Shirai [(1)], T. Fujimori [(2)], M. Kikuchi [(3)]

[(1)] *Associate Professor, Hokkaido University, shirai.kazutaka@eng.hokudai.ac.jp*
[(2)] *Senior Engineer, Obayashi Corporation, fujimori.takeshi@obayashi.co.jp*
[(3)] *Professor, Hokkaido University, mkiku@eng.hokudai.ac.jp*

Abstract

In general, if the damper characteristics of passive control systems, such as the yield strength of hysteretic dampers, are set to their optimal values, their peak response during an earthquake can be minimized. Understanding optimal damper characteristics is useful in the seismic design of vibration control structures. Additionally, it is known that soil–structure interaction (SSI) significantly affects structures' earthquake responses. The impact of SSI on seismic response is therefore an important issue in the seismic design of structures. Despite the importance of these factors, few previous studies have investigated the optimal damper characteristics of vibration control systems while considering SSI effects.

In the present study, to determine the optimal damper characteristics of passive systems considering SSI, a series of shaking table tests were conducted using a vibration control structure model with a sway–rocking mechanism under the superstructure. To investigate the optimal damper characteristics, which are the values that effectively minimize the peak response, a simple friction damper device that allows the slip force to be easily set to various magnitudes using rubber bands and stainless plates was used in the shaking tests. The test results yielded the optimal slip force characteristics of the friction damper, which were found to vary according to the sway–rocking conditions and the level of input motion.

Keywords: Earthquake response; Friction damper; Sway–rocking model

1. Introduction

In general, if the damper characteristics of passive vibration control systems, such as the yield strength of hysteretic dampers, are set to their optimal values, their peak response during an earthquake can be minimized [1, 2]. Understanding optimal damper characteristics is useful in the seismic design of vibration control structures. Additionally, it is known that soil–structure interaction (SSI) significantly affects the earthquake response of structures. The impact of SSI on seismic response is therefore an important issue in the seismic design of structures. Despite the importance of these factors, few previous studies [3, 4] have investigated the optimal damper characteristics of vibration control systems while considering SSI effects.

The objective of the present study was to determine the optimal damper characteristics of passive control systems considering SSI effects. A series of shaking table tests [5, 6] were conducted using a vibration control structure specimen with a sway–rocking (SR) mechanism under the superstructure. The remainder of this paper is organized as follows. Section 2 describes the specimens used in the shaking table tests. Section 3 outlines the experimental methods used in the free vibration and shaking table tests. The results of the shaking table tests are presented in Section 4, and Section 5 concludes the paper.

2. Test Specimen

2.1 Main frame and sway–rocking component

Fig. 1 shows the vibration control structure model and the SR component installed under the superstructure that were designed and manufactured for use in the shaking table tests. The main frame of the specimen is composed of four stainless steel plates acting as columns and a rigid beam on top of these plates. The SR component consists of linear guides and horizontal tensile coil springs for sway motion and pin parts and compression coil springs for rocking motion. Moreover, one and two commercial oil dampers were installed to dampen the sway and rocking motions of the SR component, respectively. Table 1 gives the specifications of the specimen.

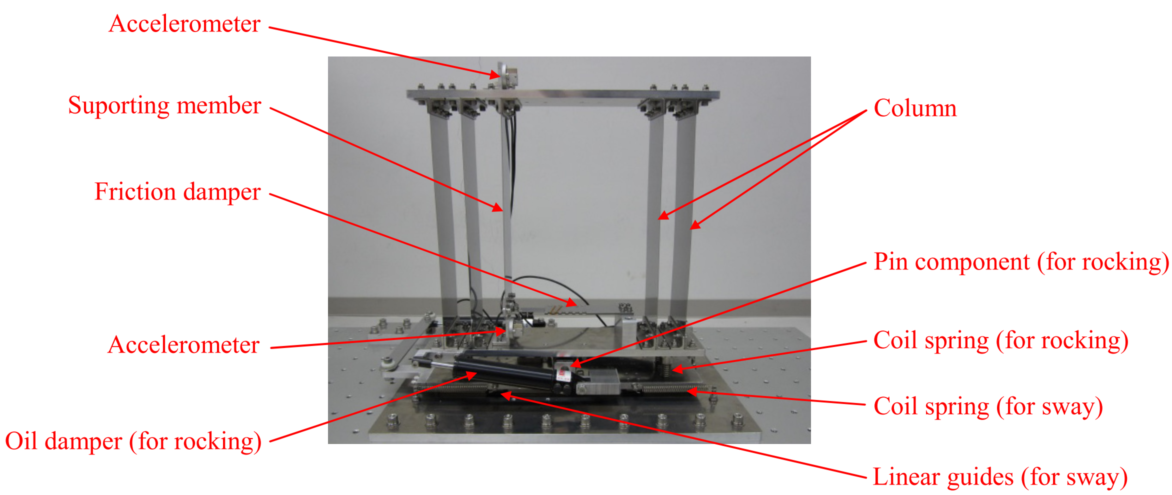

Fig. 1 – Specimen [5]

2.2 Specimen design after full-scale building

The specimen was modeled based on a design example of a full-scale reinforced concrete building (six-stories, beam–column frame structure, pile foundation) in which SSI effects were taken into consideration [7]. As shown in Table 2, the specimen was designed for each type of SSI motion (sway, rocking, and SR) such that the natural period and damping ratios of the specimen obtained by complex eigenvalue analysis were approximately the same as those of the full-scale building, the stiffness of which was the secant stiffness at its yield point.

Table 1 – Specimen specifications [5]

Property	**Component**	**Method***	**Value**
height (top to pin component)	main frame	1	0.39 m
horizontal stiffness	main frame	3	1.48 N/cm
mass (upper half)	main frame	1	2.58 kg
moment of inertia (upper half)	main frame	2	344 kg cm^2
mass	base	1	5.56 kg
moment of inertia	base	2	482 kg cm^2
horizontal stiffness	sway component	2	4.92 N/cm
horizontal damping coefficient	sway component	2	0.224 Ns/cm
rotational stiffness	rocking component	3	4.10×10^4 Ncm/rad
rotational damping coefficient	rocking component	2	740 Nscm/rad

*Method 1: direct measurement
Method 2: calculation from sizes of members and catalog specifications
Method 3: calculation from natural periods obtained in free vibration tests (Table 3)

Table 2 – Natural period and damping ratios obtained by complex eigenvalue analysis [5]

Ratio*	**Full-scale building**	**Specimen**
T_{SW}/T_F	1.19	1.24
T_{RO}/T_F	1.01	1.03
T_{SR}/T_F	1.19	1.25
h_{SW}	5.14%	6.57%
h_{RO}	0.05%	0.35%
h_{SR}	5.06%	6.30%

*T_F : natural period with fixed base
T_{SW} : natural period under sway motion
T_{RO} : natural period under rocking motion
T_{SR} : natural period under SR motion
h_{SW} : damping ratio under sway motion
h_{RO} : damping ratio under rocking motion
h_{SR} : damping ratio under SR motion

2.3 Friction damper

Fig. 2 shows the simple friction damper device composed of rubber bands and stainless plates used in the shaking table tests to determine the optimal damper characteristics, which are the characteristics that most effectively minimize the peak response. The friction damper allowed the slip force to be easily set to various magnitudes. The friction damper was connected in series to a supporting member composed of a stainless steel plate and incorporated into the superstructure of the specimen.

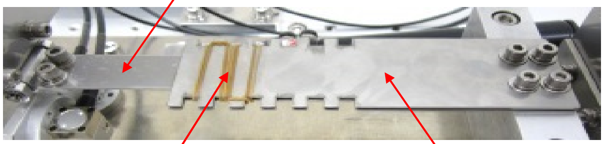

Fig. 2 – Proposed friction damper [5]

3. Methods

3.1 Free vibration tests

Free vibration tests were conducted under each type of SSI motion with each possible friction damper condition before the shaking table tests. Table 3 gives the natural periods and damping ratios obtained from the free vibration tests. The ratio of the stiffness of the supporting member connected in series to the friction damper to that of the main frame was $K_B/K_F = 1.50$ in the horizontal direction.

Table 3 – Results of free vibration tests [5]

SSI motion		Friction damper condition	Natural period [s]	Damping ratio [%]
Sway	**Rocking**			
fixed	fixed	damper fixed	0.52	0.26
fixed	fixed	no damper	0.83	0.27
fixed	movable	no damper	0.85	0.31
non-fixed*	fixed	no damper	0.88	0.25
non-fixed*	movable	no damper	0.91	0.31

* The sway component of the specimen did not move because of the initial resistance force of the linear guides.

3.2 Shaking table tests

3.2.1 Shaking table and measurement procedure

A unidirectional shaking table (maximum payload 1000 N, maximum shaking acceleration 1 G, table size 1000 mm × 500 mm) was used for the shaking table tests. The response accelerations were measured by strain-type accelerometers attached to typical parts of the specimen and the shaking table. The response displacements were calculated by the second order integration of the acceleration data.

3.2.2 Input earthquake motions

Five simulated earthquake waves (Waves L1–L5) were used as input motions. Fig. 3 shows examples of the velocity response spectra observed on the shaking table during the shaking table tests for the same wave with different input levels (Wave L1, fixed base). Each input motion was fitted to the same target acceleration response spectrum. The time axis of each input motion was adjusted such that the ratio of the corner period of the response spectrum to the natural period of the specimen agreed with that of the full-scale building. The envelope functions proposed by Amin and Ang [8] were used. The duration of the steady part of each wave was 42 s. The phase angles for each wave were set to random values.

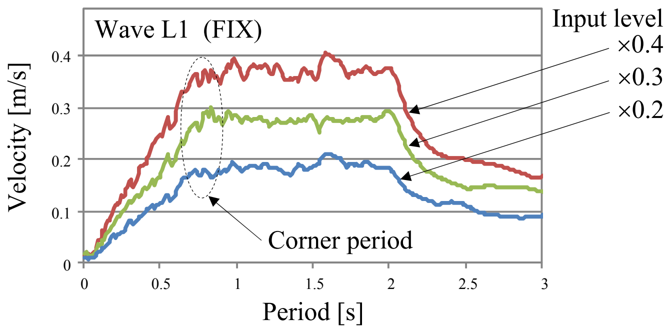

Fig. 3 – Velocity response spectra of input motions (damping factor of 5%) [6]

3.2.3 Test parameters

The main test parameters were the different SSI motions (FIX: fixed base, SR: sway–rocking), the slip force of the friction damper (approximately 13 levels, e.g., zero, moderate force, excessive force), input waves (Waves L1–L5), and input levels (i.e., multiplying factors of input motions of 0.2, 0.3, and 0.4). A total of 374 shaking tests were conducted.

In the present study, the slip forces measured during preliminary static tensile tests using spring balances (Fig. 4) under various friction damper settings (Fig. 5) were adopted as the damper slip forces.

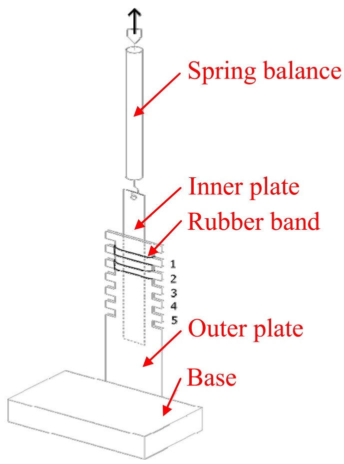

Fig. 4 – Preliminary tensile tests on friction damper using spring balances

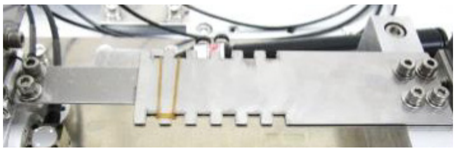

(a) Slip force: 0.35 N

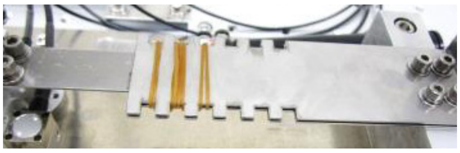

(b) Slip force: 1.65 N

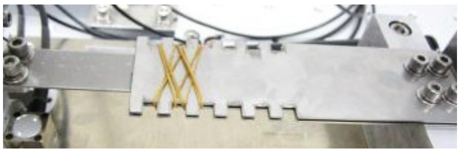

(c) Slip force: 2.25 N

Fig. 5 – Examples of friction damper settings [6]

4. Shaking Table Test Results

4.1 Response behavior

Fig. 6 shows examples of the acceleration response time history measured by the accelerometers placed at typical points on the specimen and the shaking table. Fig. 7 shows examples of response hysteresis loops for the superstructure of the specimen. From Fig. 7(b), the friction damper adopted in the present study exhibited an approximately bilinear shape.

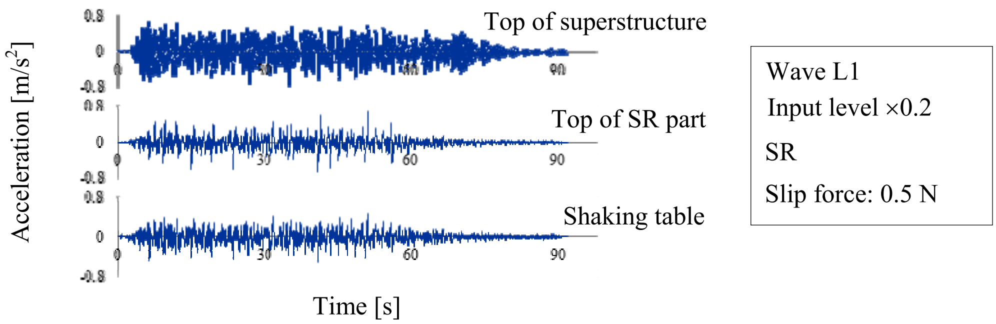

Fig. 6 – Examples of acceleration response time history [6]

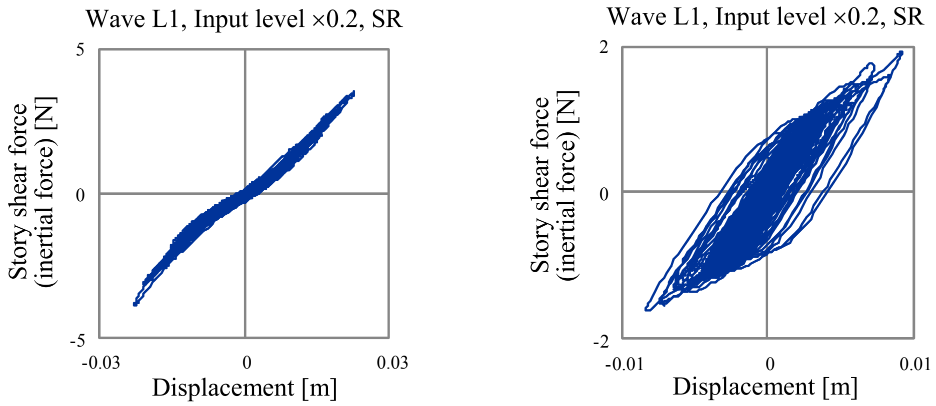

(a) Damper slip force: 0.0 N (b) Damper slip force: 0.75 N

Fig. 7 – Hysteresis loops of superstructure [6]

4.2 Optimal damper characteristics

Fig. 8 and 9 shows the relationships between the maximum response accelerations at the top of the superstructure and the damper slip forces under FIX and SR motion, respectively. In Fig. 8 and 9, each solid line represents the mean of the five input motions (Waves L1–L5). From these results, as the input level increased, the optimal damper slip force, which is the force that minimizes the maximum response, increased. The optimal damper slip force under SR motion was slightly larger than that under FIX motion. The maximum response acceleration at the optimal slip force point of the structure under SR motion was slightly lower than that under FIX motion. These results demonstrate that the optimal damper characteristics vary depending on the SR conditions.

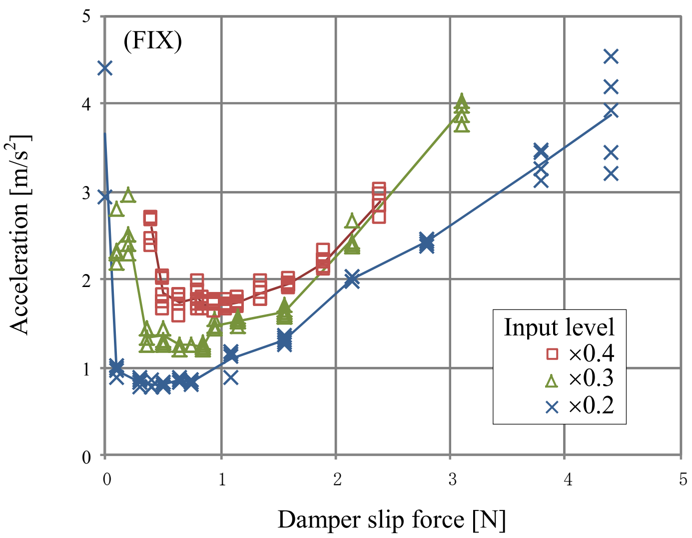

Fig. 8 – Maximum response acceleration at top of superstructure plotted against damper slip force (FIX) [6]

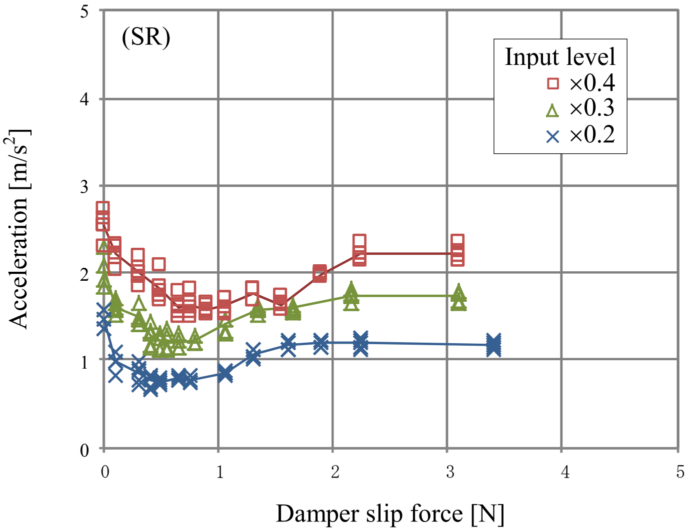

Fig. 9 – Maximum response acceleration at top of superstructure plotted against damper slip force (SR) [6]

5. Conclusion

In the present study, to determine the optimal damper characteristics of a passive vibration control system experiencing SSI, a series of shaking table tests were conducted using a vibration control structure model with an SR mechanism under the superstructure.

To determine the optimal damper characteristics, which are the values that effectively minimize the peak response, a simple friction damper device that allows the slip force to be easily set to various magnitudes using rubber bands and stainless steel plates was used for the shaking table tests. A total of 374 shaking tests were conducted. The results of the tests demonstrate that the optimal slip force characteristics of the friction damper vary depending on the SR conditions and the input level of the ground motion.

6. Acknowledgements

The authors would like to thank Ms. Akari Nagaoka, Mr. Tomonori Koya, and Mr. Toshiro Iida, who were graduate students at Hokkaido University while this study was being conducted. The present study was supported by JSPS KAKENHI Grant Numbers JP 24760441 and JP 16K06564. The authors also gratefully acknowledge the research grant from the Toda Scholarship Foundation (2013).

7. References

[1] Shirai K, Kageyama M, Ikago K, Inoue N (2011): Study on optimum damper yield strength based on transfer function of equivalent linear system for R/C structure with hysteretic damper. *Journal of structural and construction engineering*, *Architectural Institute of Japan*, **76** (666), 1433-1442. (In Japanese)

[2] Shirai K, Kageyama M, Ikago K, Inoue N (2013): Optimum Yield Strength of a Hysteretic Damper Incorporated into RC Structures Using the Transfer Function of an Equivalent Linear System. *13th World Conference on Seismic Isolation, Energy Dissipation and Active Vibration Control of Structures* (*13WCSI*), 120, 1-8, Sendai, Japan.

[3] Tsuruga T, Motosaka M (2000): Optimal Damper Placement for Soil-Structure Interaction System. *Research reports of AIJ Tohoku Branch*, *Architectural Institute of Japan*, (63), 149-152. (In Japanese)

[4] Koya T, Shirai K, Fujimori T, Kikuchi M (2013): Optimum Damping Characteristic Evaluation of Vibration Control System with Maxwell Damper in Consideration of Soil-Building Interaction. *Summaries of technical papers of annual meeting 2013*, *Architectural Institute of Japan*, B-2, 969-970. (In Japanese)

[5] Shirai K, Nagaoka A, Koya T, Fujimori T, Kikuchi M (2014): Experimental Study on Optimum Damper Characteristics of Passive Control Structures Considering Soil-Structure Interaction Part 1 Design of a Specimen. *Summaries of technical papers of annual meeting 2014*, *Architectural Institute of Japan*, B-2, 13-14. (In Japanese)

[6] Nagaoka A, Shirai K, Fujimori T, Kikuchi M (2014): Experimental Study on Optimum Damper Characteristics of Passive Control Structures Considering Soil-Structure Interaction Part 2 Methods and Results of Shake Table Tests. *Summaries of technical papers of annual meeting 2014*, *Architectural Institute of Japan*, B-2, 15-16. (In Japanese)

[7] Architectural Institute of Japan (2006): *Seismic Response Analysis and Design of Buildings Considering Dynamic Soil-Structure Interaction*. 205-240. (In Japanese)

[8] Amin M, Ang A H-S (1968): Nonstationary stochastic model of earthquake motions. *Journal of the Engineering Mechanics Division*, *ASCE*, 94, EM2, 559-583.